

# Evaluation of the Impact of AIRS Radiance and Profile Data Assimilation in Partly Cloudy Regions

Bradley Zavodsky\*, Jayanthi Srikishen<sup>†</sup>, Gary Jedlovec\*

\*NASA/Marshall Space Flight Center, Huntsville, AL

<sup>†</sup>Universities Space Research Association, Huntsville, AL

## ABSTRACT

Improvements to global and regional numerical weather prediction have been demonstrated through assimilation of data from NASA's Atmospheric Infrared Sounder (AIRS). Current operational data assimilation systems use AIRS radiances, but impact on regional forecasts has been much smaller than for global forecasts. Retrieved profiles from AIRS contain much of the information that is contained in the radiances and may be able to reveal reasons for this reduced impact. Assimilating AIRS retrieved profiles in an identical analysis configuration to the radiances, tracking the quantity and quality of the assimilated data in each technique, and examining analysis increments and forecast impact from each data type can yield clues as to the reasons for the reduced impact. By doing this with regional scale models individual synoptic features (and the impact of AIRS on these features) can be more easily tracked. This project examines the assimilation of hyperspectral sounder data used in operational numerical weather prediction by comparing operational techniques used for AIRS radiances and research techniques used for AIRS retrieved profiles. Parallel versions of a configuration of the Weather Research and Forecasting (WRF) model with Gridpoint Statistical Interpolation (GSI) are run to examine the impact AIRS radiances and retrieved profiles. Statistical evaluation of a long-term series of forecast runs will be compared along with preliminary results of in-depth investigations for select case comparing the analysis increments in partly cloudy regions and short-term forecast impacts.

## 1. MOTIVATION

Since the launch of the Aqua satellite in 2002, assimilation of radiances from the Atmospheric Infrared Sounder (AIRS; Aumann et al. 2003) has resulted in positive impact on numerical weather prediction (NWP) (e.g. McNally et al. 2006, LeMarshall et al. 2006, McCarty et al. 2009). As a result, radiance observations from AIRS have been operationally assimilated into both global models, such the National Centers for Environmental Prediction (NCEP) Environmental Modeling Center (EMC) Global Forecast System (GFS) and European Centre for Medium-Range Weather Forecasts (ECMWF), and regional models, such as NCEP EMC's North American Mesoscale (NAM). NCEP's global and regional systems both use the Gridpoint Statistical Interpolation (GSI; Wu et al. 2001) as their operational data assimilation system.

Current assimilation strategies for AIRS radiances only use cloud-free radiances from a 281-channel subset of the full 2378 channels (LeMarshall et al 2006). In addition, data are thinned to 120-km resolution (1 out of every 81 spatial footprint) in the regional system (Derber 2010). Because of these spectral and spatial

thinning techniques, less than 1% of the total AIRS volume is used in the assimilation process (Goldberg et al. 2003). McCarty et al. (2009) demonstrated the importance of using more observations (spatially) within regional scale applications to capture synoptic patterns that might be missed by observations with larger horizontal spacing. This work also demonstrated that current cloud detection methodologies within the Community Radiative Transfer Model (CRTM; Han et al. 2006) may misplace the vertical extent of clouds in some instances leading to either 1) further reduction of clear radiances above cloud tops or 2) introduction of cloud-contaminated radiances.

The objective of the work described herein is to use AIRS Level 2 retrieved temperature and moisture profiles to better understand the optimal three-dimensional distribution of AIRS radiances assimilated within GSI to engage the operational data assimilation community in discussion to optimize strategies for assimilating hyperspectral radiances. The Level 2 data contain the same information content as the radiances; however, through cloud clearing and error checking an estimate of where quality data from AIRS is possible can be found (Susskind 2006). Comparing the vertical pressure level

above which quality observations are found in the retrieved profiles and the cloud top pressure (CTP) determined by CRTM using cloud information from the Moderate resolution Infrared Spectroradiometer (MODIS) as a “ground truth”, this paper will focus on how well the CRTM within GSI determines cloud-free radiances.

This work is conducted as a collaborative effort between the Joint Center for Satellite Data Assimilation (JCSDA) and Short-term Prediction Research and Transition (SPoRT) Center.

## 2. EXPERIMENT SETUP

Two parallel 4-week experiments with a 2-week spin-up were performed to test the impact of AIRS radiances and profiles on a version of the Weather Research and Forecasting (WRF; Skamarock et al. 2007) Nonhydrostatic Mesoscale Model (NMM) designed to mimic the operational NAM. The regional, 4-km resolution NAM system was used here for two reasons. First, the higher resolution domain allowed for assimilation of a larger amount of data without running into horizontal correlation discrepancies. Second, the 4-km resolution allowed for some cloud-resolving capabilities, which made for more detailed analysis of how CRTM and GSI designate CTP compared to MODIS.

Figure 1 illustrates the methodology of the NAM cycling, which involves 12 hour spin-up cycles prior to each analysis time (00, 06, 12, and 18 UTC) whereby data valid at each time

are assimilated. Each pre-cycle consists of a series of GSI analyses at 3-hour intervals with a background coming from a WRF forecast from the previous 3-hour cycle. Observational data are obtained in 3-hour bundles ( $\pm 1.5$  hours) and assigned a “time-minus” (TM) time describing which cycle they are to be assimilated in. As an example, `ndas.t00z.airsev.tm06.bufr_d` contains AIRS radiances to be used in the 0000 UTC pre-cycle that is valid at 1800 UTC on the previous day (i.e. 6 hours before 0000 UTC). This particular cycling methodology allows for satellite data not available in real-time due to data latency to still impact the NAM in the next cycle.

For each experiment, satellite bias was set to 0.00 at the beginning of the 2-week spin-up (4-19 November 2011) and evolved as data was assimilated through the end of the 4-week case study period (20 November – 20 December 2011). All satellite (NCEP Table 19) and conventional (NCEP Table 4) observations assimilated operationally into the NAM as of late 2011 were also assimilated (See Table 1).

The WRF-NMM and GSI code used herein comes from the Developmental Testbed Center (DTC), which works collaboratively with EMC to transition its operational code to the research community. The experiments were conducted on the NASA Center for Climate Simulation (NCCS) Joint Center in a Big Box (JIBB) supercomputing system operated out of Goddard Space Flight Center and available to collaborators of the JCSDA.

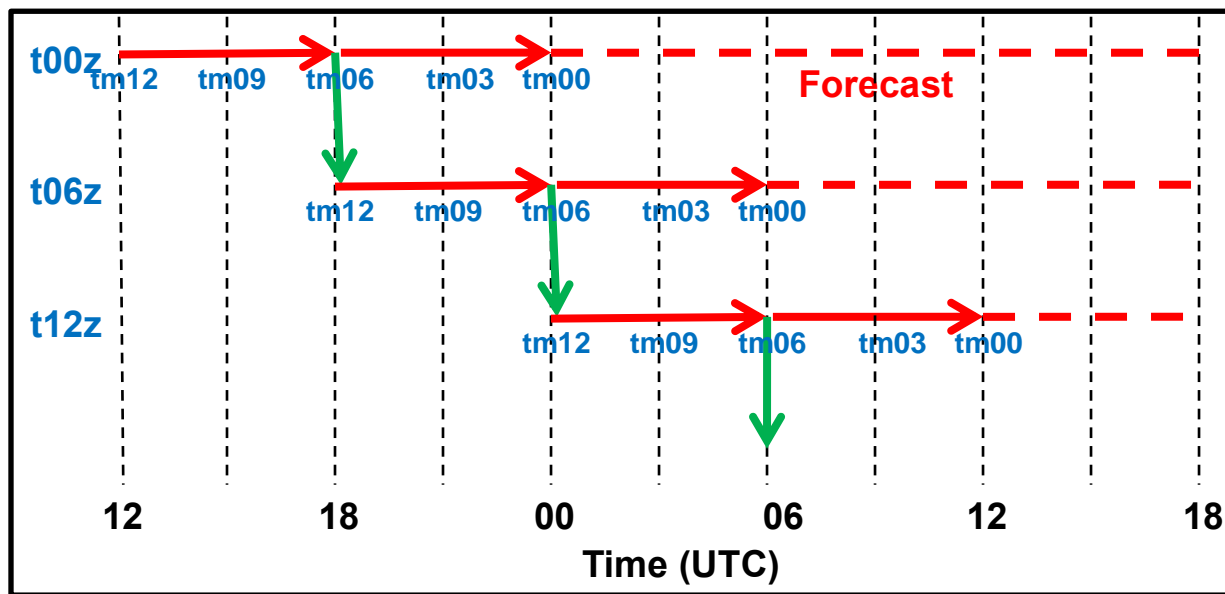


Figure 1. Schematic of operational NAM cycling methodology (DiMego, personal communication, 2011).

The AIRS radiance experiment (RAD) used all of the operational satellite and conventional datasets plus the AIRS Level 1B radiance data. Observation errors were identical to those used in the operational system. The AIRS profile experiment (PRO) used all of operational satellite and conventional datasets but instead of the AIRS radiances, AIRS retrieved temperature and moisture profiles were assimilated. The AIRS profiles were assimilated by appending the conventional PREPBUFR files and treating them as radiosondes. Because of the way GSI introduces observation errors, the AIRS profiles assimilated as radiosondes are assigned observation errors that match the radiosonde observation errors. In the preprocessing of the AIRS retrieved profiles, the quality flag,  $P_{best}$ , was used to select data only the best data in the vertical for assimilation. Because  $P_{best}$  uses information from the cloud-cleared radiances, it represents the amount of information that could be available from AIRS if cloud-clearing was used in the radiance methodology. For the results presented herein, no observation thinning was performed on the retrieved profile data, meaning that the PRO experiments represent a maximum amount of information in both the horizontal and vertical that could be obtained from AIRS.

Table 1. Satellite and conventional observations assimilated in experiments

	RAD	PRO
AMSU-A	N15, N18, N19, MetOp-A, Aqua	N15, N18, N19, MetOp-A, Aqua
MHS	N18, MetOp-A	N18, MetOp-A
HIRS	N17, N19, MetOp-A	N17, N19, MetOp-A
Sounder	GOES11, GOES12	GOES11, GOES12
<b>AIRS</b>	<b>L1B radiances</b>	<b>L2 T and q profiles</b>
Conventional	Sondes, Aircraft, SatWinds, METAR, BUOY	Sondes, Aircraft, SatWinds, METAR, BUOY

### 3. Overall Case Study Results

As mentioned in Section 2, a 4-week case study period from 20 November to 20 December 2011 was used to investigate the impact of assimilated AIRS observations on regional forecasts. Forecast impact on 500 hPa height and temperature anomaly correlation coefficients (ACC) were used to evaluate regions where the profiles had the largest positive forecast impact. These regions were then compared to MODIS CTP and effective cloud fraction (ECF) for regions to perform further investigations.

ACC is a measure of the quality of a forecast system that subtracts out a climatological average from both the forecast and analysis used for verification. It is calculated as:

$$ACC = \frac{\overline{(f - c)(a - c)}}{\sqrt{\overline{(f - c)^2(a - c)^2}}}$$

where  $f$  is the model forecast value,  $a$  is the verifying analysis value, and  $c$  is a climatology value. Here, the verifying analysis,  $a$ , was the same-cycle analysis valid from each experiment at the forecast time. The climatology values,  $c$ , were taken from the NCEP reanalysis climatology used by EMC to calculate ACC for their forecast systems, and interpolated using a nearest-neighbor approach, to the NAM 4-km grid.

Figure 2 shows 500 hPa height and temperature ACC differences between the

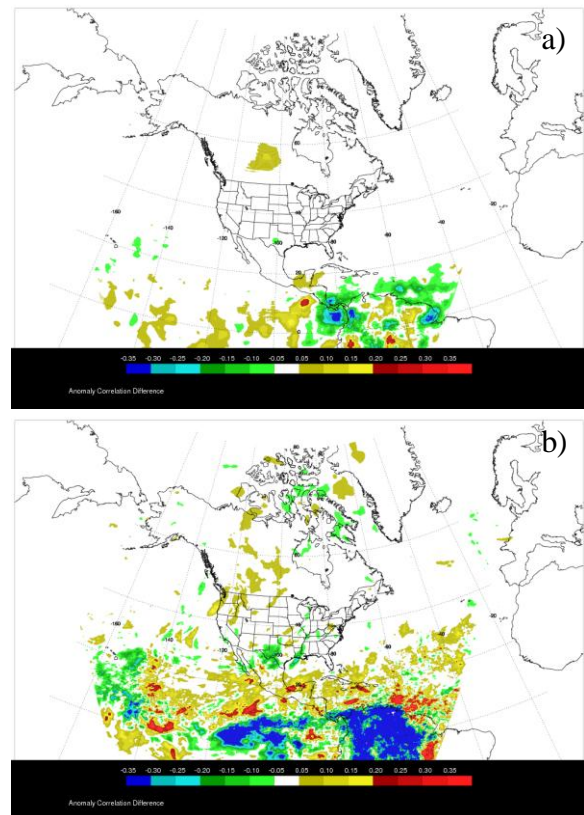


Figure 2. 500 hPa a) height and b) temperature ACC differences between radiance assimilation and profile assimilation (RAD-PRO) on a grid point-to-grid point basis for all 48-hr forecasts initialized at the 0000 UTC cycle for the 20 November to 19 December case study period.

radiance and profile 48-hr forecasts. The difference is RAD minus PRO; thus, larger ACC values (i.e. better forecasts) for the PRO experiment are in the cool greens and blue and for the RAD are in warm yellows and reds. For this time period, the largest differences between the PRO and RAD experiments were in the tropics and specifically over the Intertropical Convergence Zone (ITCZ). In the Equatorial region, the PRO experiment performed much better than the RAD experiment. Between 10°S and 10°N latitude, the 500 hPa temperature ACC was 0.552 for the RAD and 0.667 for the PRO.

One of the key features of the Equatorial region is high humidity and a general presence of cloud cover. To better quantify the presence and vertical extent of cloud cover, a mean value of cloud state at each WRF grid point was derived from MODIS for the 4-week case study period. Five-kilometer resolution MODIS Cloud Product data from Aqua (MYD06\_L2) data were binned to the 4-km WRF grid using a nearest-neighbor methodology (Fig. 3). Due to its

collocation with AIRS, only MODIS data from Aqua were used to compile the mean cloud state to ensure accurate representation of cloud features at the time of AIRS overpasses. Figure 3a shows the mean ECF with warmer colors representing more overcast skies; Figure 3b shows the mean CTP with warmer colors representing lower cloud tops. From Fig. 3, there were persistent overcast skies over the North Atlantic and North Pacific that appear to be mid-level clouds. Another feature of interest was the band of clouds near the Equator and over Northwestern South America likely associated with the ITCZ. The linear band of Equatorial clouds appears to be low in the atmosphere (between 700 and 800 hPa). This region of persistent low clouds was a prime target for further investigation into the differences between the vertical extents of data assimilated to better understand the forecast impact differences between the two experiments.

#### 4. RESULTS FROM REPRESENTATIVE CASE: 22 NOVEMBER 2011

To investigate the cloud detection within the CRTM and GSI, a representative case (22 November 2011) was used. In particular, the ITCZ region over the Eastern Pacific was a focus due to the cloud features. Figure 4 shows a metric called the Impact Difference (ID), which is a measure of the difference in the analysis increment at a particular grid point. It is calculated as:

$$ID_{i,j} = \left| RADALYS_{i,j} - RADBKGD_{i,j} \right| - \left| PROALYS_{i,j} - PROBKGD_{i,j} \right|$$

where ALYS is the analysis and BKGD represents is the background for each experiment. The value is calculated on a grid point-by-grid point basis (i,j). While this measure does not provide any guidance regarding which analysis was better based on some ground truth, the assertion is that the improved ACC values in the ITCZ region means that the analysis was moved closer towards a real atmospheric state. Due to the way the metric is calculated, negative values (greens and blues in Fig. 4) indicate larger analysis increments in the PRO experiment, and positive values (yellows and reds in Fig. 4) indicate larger analysis increments in the RAD experiment.

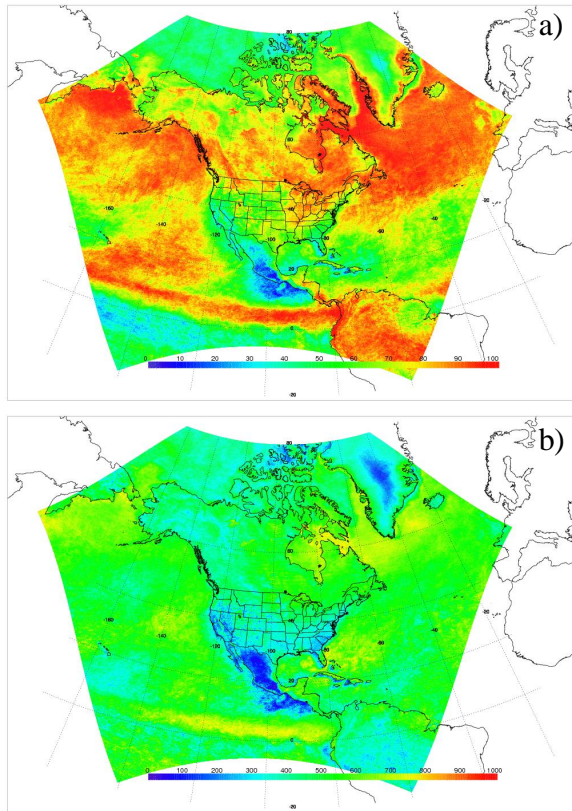


Figure 3. Mean cloud properties for the 20 November to 20 December 2011 case study period derived from the MODIS Cloud Products (MYD06\_L2) from the Aqua Satellite. Effective Cloud Fraction (ECF) is shown in a); Cloud Top Pressure (CTP) is shown in b).



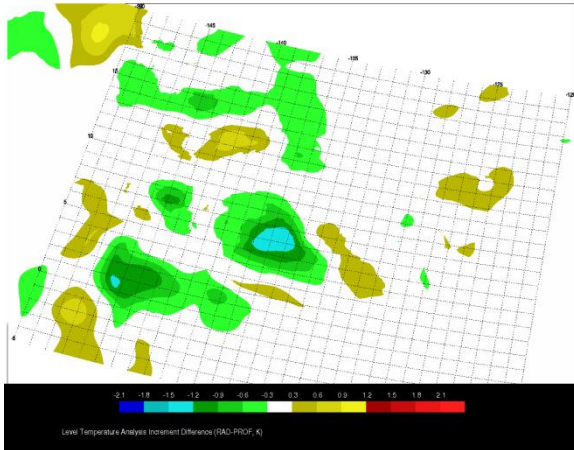


Figure 4.  $\approx 500$  hPa ( $\sigma = 39$ ) temperature ID for the 0000 UTC analysis on 22 November 2011.

For the 0000 UTC analysis on 22 November 2011, the AIRS overpass valid at that time was focused on a swath that ran from Hawaii to Alaska. Figure 4 shows the temperature ID value for a zoomed in region Southeast of Hawaii at approximately 500 hPa ( $\sigma = 39$ ) over the western edge of the low clouds. Here, there was a region of larger analysis impact from the PRO experiment on the order of 1.5 K.

Figure 5 shows the MODIS CTP product valid around 2240 UTC on 21 November 2011, coincident in time and space with the AIRS data assimilated in the 0000 UTC analysis on 22 November 2011. From the image, there were clear skies and very low-level clouds over the southern half of the swath. The northern half of the swath had high clouds with some patches of low- and mid-level clouds. The region where the ID had the largest negative value (i.e. PRO experiment had largest analysis impact compared to the RAD) occurred along the transition zone between the low and high clouds.

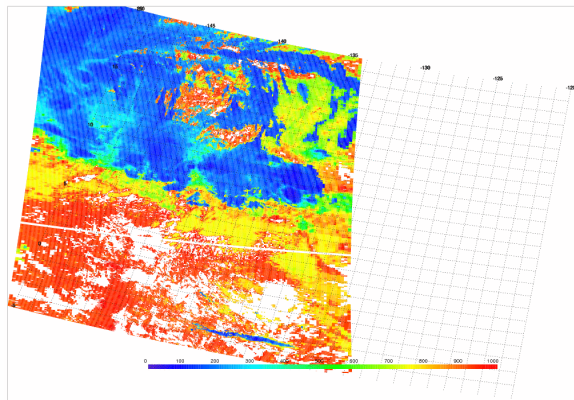


Figure 5. MODIS CTP valid around 2240 UTC on 21 November 2011.

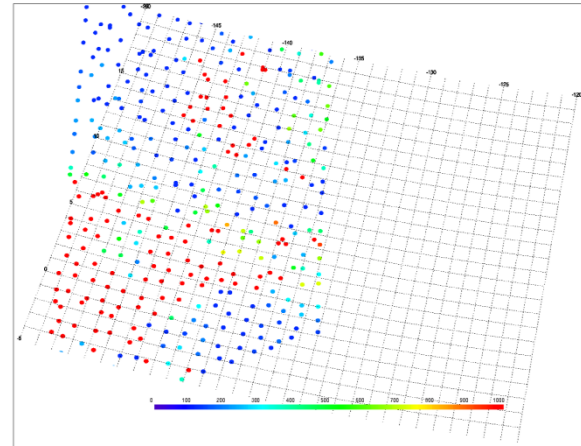


Figure 6. CTP diagnosed by CRTM/GSI at locations of assimilated AIRS radiances for 0000 UTC analysis on 22 November 2011. AIRS observations are valid at around 2240 UTC, coincident with MODIS CTP in Fig. 5.

Comparing the CTP estimates returned by CRTM/GSI for the assimilated AIRS radiances yielded pretty good agreement with the MODIS CTP. However, there were a couple of areas where the CRTM/GSI CTP was too high (altitude-wise) compared to what is observed by MODIS. In particular, the transition region between the clear skies and low clouds in the south and the high clouds in the north appeared to be mismatched. From MODIS, the CTP in this transition region appeared to be between 700 and 800 hPa, but the CRTM/GSI CTP for this same region appeared to be between 300 and 600 hPa. Matching up the regions where there was a larger analysis impact in the PRO experiment revealed that these areas also contain misrepresented CTP from CRTM/GSI. Both areas of  $<1.0$  ID values in Fig. 4 revealed clear skies and/or near-surface/low-level clouds (800-1000 hPa) in the MODIS CTP product (Fig. 5), but high clouds (300-600 hPa) in the CRTM/GSI CTP (Fig. 6).

As mentioned in Section 1, only channels that are detected as cloud-free are assimilated by GSI. Figure 7a shows the AIRS radiance locations assimilated in channel 253 ( $722.13 \text{ cm}^{-1}$ ), which peaks at 501 hPa. The locations of the assimilated AIRS radiances matched pretty closely with values of MODIS CTP greater 500 hPa except for two holes in the clear/low-cloud region in the southern half of the swath associated with the region of larger profile impact. For comparison, the data assimilated in the PRO experiment at the 500 hPa level are shown in Fig. 7b. Recall, that these data were quality controlled using the  $P_{\text{best}}$  variable, which designates the highest-quality retrievals. The

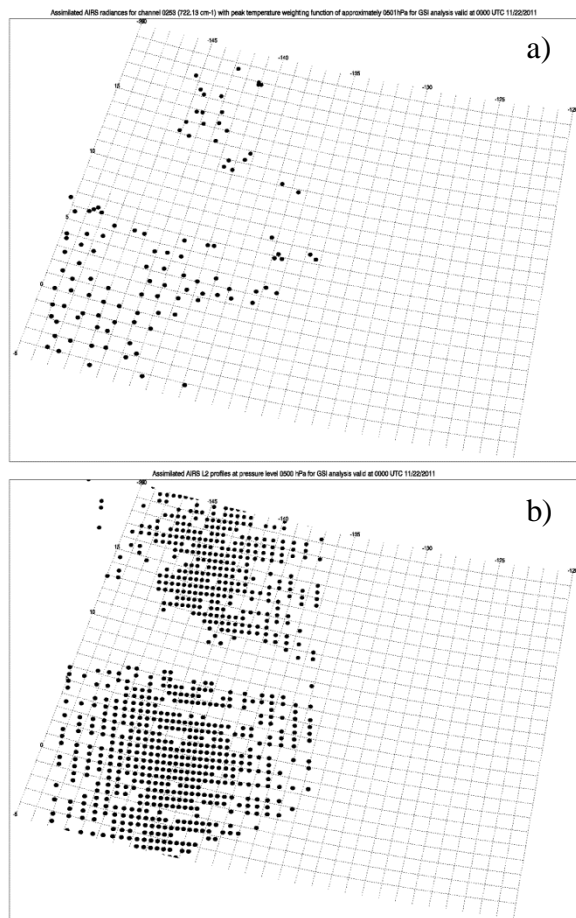


Figure 7. Locations of assimilated AIRS observations for a) channel 253 (722.13 cm<sup>-1</sup>; peak at 501 hPa) and b)  $P_{best}$  value greater than 500 hPa for 0000 UTC analysis on 22 November 2011.

assimilated profiles in the PRO experiment provided a better matchup to the CTP pattern in the MODIS data shown in Fig. 5 suggesting that there were still quality radiances from AIRS available at the 500 hPa level that could still be assimilated. Specifically, the holes in the assimilated radiance data in Fig. 7a were not present in the assimilated profile data locations in Fig. 7b.

## 5. SUMMARY AND FUTURE WORK

The preliminary results of a collaborative project between the JCSDA and SPoRT are presented. Parallel experiments assimilating AIRS radiances and profiles into a GSI/WRF-NMM configuration designed to mimic the operational NAM were performed for a 4-week case study from late 2011. Overall, the 500 hPa height and temperature ACC values in the Equatorial region were improved when profile data are assimilated instead of radiances. In

this region, MODIS detected persistent, low clouds throughout the case study time period. Comparisons of the vertical extent of the assimilated radiances and profiles in the separate experiments to MODIS observations revealed that part of the cause of the improvement in the profile forecasts is linked to reduced analysis impact from the AIRS radiances in the mid-troposphere.

Future work will focus on assimilation experiments that adjust the thinning of the AIRS profiles to retain less data and the AIRS radiances to retain more data to determine how much of the increased analysis impact from the profiles results from the larger number of assimilated observations. We will also work to “turn knobs” within the CRTM/GSI cloud detection algorithms to better understand how changes might result in a larger number of radiances being assimilated in the vertical and whether the analysis impact and forecast results are improved by addition of these radiances.

## ACKNOWLEDGMENTS

This work is supported by Tsengdar Lee of the NASA Science Mission Directorate through the JCSDA and SPoRT. The authors would like to thank the staff at EMC (Geoff DiMego, Justin Cooke, Michael Lueken, et al.) for helping with our understanding of the cycling, configuration of our system that mimics the operational NAM, and making NAM BUFR observations available to the research community at our request. We would also like to thank the JIBB IT staff for allowing us to run our simulation and store our large analysis and forecast files on these NASA supercomputing resources. Finally, we would like to thank Fanglin Yang of EMC for providing the climatology files used by EMC for calculating anomaly correlations.

## REFERENCES

- Aumann, H. H., M. T. Chahine, C. Gautier, M. D. Goldberg, E. Kalnay, L. M. McMillin, H. Revercomb, P. W. Rosenkranz, W. L. Smith, D. H. Staelin, L. L. Strow, and J. Susskind, 2003: AIRS/AMSU/HSB on the Aqua Mission: Design, Science Objectives, Data Products, and Processing Systems. IEEE Transactions on Geoscience and Remote Sensing, 41, 253-264.
- Derber, J. C., 2010: Overview of GSI. Gridpoint Statistical Interpolation Community Tutorial,

Boulder, CO. [Available online at:  
[http://www.dtcenter.org/com-GSI/users/docs/presentations/2010\\_tutorial/L2-0628-GSI\\_Overview\\_JohnDerber.ppt.pdf](http://www.dtcenter.org/com-GSI/users/docs/presentations/2010_tutorial/L2-0628-GSI_Overview_JohnDerber.ppt.pdf)]

Goldberg, M. D., Y. Qu, L. M. McMillin, W. Wolf, Z. Lihang, and M. Divakarla, 2003: AIRS near-real-time products and algorithms in support of operational numerical weather prediction. *IEEE Trans. Geosci. Remote Sens.*, **41**(2), 379-399.

Han, Y. P. van Delst, Q. Liu, F. Weng, B. Yan, R. Treadon, and J. Derber, 2006: JCSDA Community Radiative Transfer Model (CRTM) version 1, Tech. Rep. 122, NOAA, Washington, D.C. [Available online at:  
[http://www.emc.ncep.noaa.gov/research/JointOSSEs/Manuals/CRTM\\_v1\\_NOAAtechReport.pdf](http://www.emc.ncep.noaa.gov/research/JointOSSEs/Manuals/CRTM_v1_NOAAtechReport.pdf)]

Le Marshall, J., J. Jung, J. Derber, M. Chahine, R. Treadon, S. J. Lord, M. Goldberg, W. Wolf, H. C. Liu, J. Joiner, J. Woollen, R. Todling, P. van Delst, and Y. Tahara, 2006: Improving Global Analysis and Forecasting with AIRS. *Bull. Amer. Met. Soc.*, **87**, 891-894.

McCarty, W. M., G. J. Jedlovec, T. L. Miller, 2009: Impact of the assimilation of Atmospheric Infrared Sounder radiance measurements on short-term weather forecasts. *J. Geophys. Res.*, **114**, D18122, doi: 10/1029/2008JD011626.

McNally, A. P., P. D. Watts, J. A. Smith, R. Engelen, G. A. Kelly, J. N. Thépaut, and M. Matricardi, 2006. The assimilation of AIRS radiance data at ECMWF. *Quart. J. Roy. Meteor. Soc.*, **132**, 935-957.

Skamarock, W. C., J. B. Klemp, J. Dudhia, D. O. Gill, D. M. Barker, M. G. Duda, X-Y. Huang, W. Wang and J. G. Powers, 2008: A Description of the Advanced Research WRF Version 3, NCAR Technical Note, NCAR/TN-475+STR, 123 pp. [Available online at  
[http://www.mmm.ucar.edu/wrf/users/docs/arw\\_v3.pdf](http://www.mmm.ucar.edu/wrf/users/docs/arw_v3.pdf)]

Susskind, J., 2006: Improved soundings and error estimates using AIRS/AMSU data.

*Proc. SPIE Int. Soc. Opt. Eng.*, 6233, **19**, 12 pp.

Wu, W.-S., R. J. Purser, and D. F. Parrish, 2002: Three-dimensional variational analysis with spatially inhomogeneous covariances. *Mon. Wea. Rev.*, **130**, **12**, 2905-2916.